



This is a repository copy of *Modifications to the spreading resistance equation when using micro-contact impedance spectroscopy to measure resistive surface layers.*

White Rose Research Online URL for this paper:

<https://eprints.whiterose.ac.uk/216225/>

Version: Accepted Version

---

**Article:**

Ma, H., Sinclair, D.C. [orcid.org/0000-0002-8031-7678](https://orcid.org/0000-0002-8031-7678) and Dean, J.S. [orcid.org/0000-0001-7234-1822](https://orcid.org/0000-0001-7234-1822) (2024) Modifications to the spreading resistance equation when using micro-contact impedance spectroscopy to measure resistive surface layers. *Solid State Ionics*, 414. 116652. ISSN 0167-2738

<https://doi.org/10.1016/j.ssi.2024.116652>

---

© 2024 The Authors. Except as otherwise noted, this author-accepted version of a journal article published in *Solid State Ionics* is made available via the University of Sheffield Research Publications and Copyright Policy under the terms of the Creative Commons Attribution 4.0 International License (CC-BY 4.0), which permits unrestricted use, distribution and reproduction in any medium, provided the original work is properly cited. To view a copy of this licence, visit <http://creativecommons.org/licenses/by/4.0/>

**Reuse**

This article is distributed under the terms of the Creative Commons Attribution (CC BY) licence. This licence allows you to distribute, remix, tweak, and build upon the work, even commercially, as long as you credit the authors for the original work. More information and the full terms of the licence here:

<https://creativecommons.org/licenses/>

**Takedown**

If you consider content in White Rose Research Online to be in breach of UK law, please notify us by emailing [eprints@whiterose.ac.uk](mailto:eprints@whiterose.ac.uk) including the URL of the record and the reason for the withdrawal request.



[eprints@whiterose.ac.uk](mailto:eprints@whiterose.ac.uk)  
<https://eprints.whiterose.ac.uk/>

# Modifications to the spreading resistance equation when using micro-contact impedance spectroscopy to measure resistive surface layers.

Hong Ma<sup>1,2</sup>, Derek C. Sinclair<sup>1</sup> and Julian S. Dean<sup>1</sup>

1. Department of Materials Science and Engineering, Sir Robert Hadfield Building, Mappin Street, Sheffield S1 3JD, UK
2. Institute of Process Engineering, Chinese Academy of Sciences, Beijing 100190, PR China

## Abstract:

Micro-contact impedance spectroscopy (mcIS) is a powerful tool that can allow local features such as grain boundaries and surfaces in electro-ceramics to be directly interrogated. Typical macroscopic electrodes fully cover the specimen surfaces and data are converted from resistance into conductivity using a geometric correction factor based on the surface area of the electrodes and thickness of the sample. For mcIS measurements this requires a different approach. The conversion factor required in this case is that for a spreading resistance and the correction factor depends on the radius ( $r$ ) and separation of the micro-contacts. When dealing with conversions for samples with a resistive surface layer, two extreme scenarios exist depending on the thickness of the surface layer ( $T$ ) and the arrangement and size of the contacts. When the resistive layer is thin ( $T/r < 10$ ) the geometric correction factor provides accurate conductivities but for thick layers ( $T/r > 10$ ) the spreading resistance correction equation is required. When the surface layer is an intermediate thickness however neither provides a good estimate for conductivity.

Using finite element modelling we simulate resistive surface layer systems using a top-top micro-contact arrangement and show that instead of using either of the two separate correction equations, a single modified spreading resistance equation can be used on the resulting impedance data to provide greater accuracy and simplicity in the extraction of conductivity. With this modified correction factor, we show that when the ratio of bulk material conductivity versus surface layer conductivity ( $\sigma_b/\sigma_s$ ) is  $\geq 100$ ,  $\sigma_s$  can be calculated for any surface layer thickness. When the ratio is  $< 100$ , only when  $(T/r)$  is  $> 3$  can  $\sigma_s$  be accurately estimated.

## Introduction

A particular strength of impedance spectroscopy (IS) in the study of ceramics is its ability to separate contributions from electrically distinct regions, such as the bulk (grains) and grain boundaries [1]. The typical experimental setup uses two macroscopic electrodes that completely cover the upper and lower surfaces of a sample and therefore probe the electrical response(s) through the entire specimen [2,3]. To convert the raw data from resistance to conductivity, a geometric correction factor is used as shown in Equation 1 where  $R$  is the measured resistance and  $A$  is the electrode area.

$$\sigma = \frac{t}{RA} \quad (1)$$

The variable  $t$  is the thickness of the sample but note in this case this is the distance between the electrodes if the electrodes cover the full top and bottom surfaces of the

sample.

Using conventional IS in electro-ceramics becomes challenging if the geometry of an electro-active region is unknown. Although sample dimensions can be used to correct data for bulk values if a thin resistive surface is present, the thickness of this region is required to accurately correct the surface resistance into surface conductivity. This generally requires methods such as scanning and/or transmission electron microscopy that are time-consuming and where sample preparation methods can alter the properties and thickness of the surface.

One method to overcome this is by reconfiguring the contacts using micro-contact impedance spectroscopy (mclS). These measurements take place in local regions of the sample surface and a typical mclS in top-top configuration uses an array of discrete micro-contacts on the surface of a sample/device, generally of radius ranging between  $r = 5\text{-}20\ \mu\text{m}$  and separated by distance  $S$ . This technique has previously been used to characterise surface layers, individual grains and grain boundaries in various ceramics and thick/thin films [4-10]. In a top-top configuration, it has been shown that 75% of the impedance response originates from a region that extends four times the micro-contact radius into the surface of the material [6]. This does however induce greater complexity into the data correction and analysis. As the current spreads out from these contacts, a modification to the geometric factor is required to correct the geometry to establish the conductivity. Assuming there is no confinement or interference to the current density, the relationship between the resistance and conductivity can be given as

$$\sigma = \frac{1}{2r} \frac{1}{R_{Spr}} \quad (2)$$

where  $R_{Spr}$  is the measured spreading resistance and  $r$  is the micro-contact radius. Note that in this form, there is a correction factor of  $1/2$  and that the resistance does not depend on the proximity of the two contacts. A schematic of this type of spreading is shown in Figure 1.

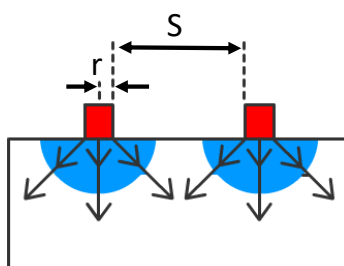


Figure 1. A schematic of the current spreading from two micro-contacts of radius  $r$  and separation  $S$ , on a homogenous and isotropic material with negligible confinement or interference in the configuration.

In many cases we desire to understand the properties of the bulk material and surface features such as cracks, roughness and changes in the surface properties are unwanted. Sample preparation such as polishing can remove these features to overcome these issues but in this article we focus on this technique being used to determine the properties of a resistive layer on the surface of a bulk region.

The mclS technique has been used by Fleig and Maier [5] to measure the conductivity of surface layers in AgCl. However, instead of a direct measurement of the surface layer conductivity, the material properties were inferred through changes in the signal

compared to the bulk response. Navickas [7] also used mclS to characterise yttria-stabilized zirconia thin films (YSZ) (20-90 nm in thickness) on a Silicon substrate. In this work they used a standard geometric correction factor such as in equation 1, to estimate the conductivity of the layer. Joo and Choi [8] also used mclS to investigate the conductivity of YSZ thick films (0.2-1.5  $\mu\text{m}$ ) on Pt substrates. The impedance data showed both the across-plane and in-plane conductivity of YSZ thick films are close to YSZ bulk specimens; however, throughout they also used the standard geometric factor equation to correct for geometry.

The mclS technique has also been widely used in the characterisation of thermal barrier coatings on superalloys. Thermal barrier coatings generally have lower conductivity than the superalloy substrate which can be considered as a two-layer or multi-layer system. A study of  $3\text{Gd}_2\text{O}_3\text{-}3\text{Yb}_2\text{O}_3\text{-}4\text{Y}_2\text{O}_3$  co-doped  $\text{ZrO}_2$  (GY-YSZ) thermal barrier coating was conducted by Zhang [9]. In this experiment, the mclS study revealed an increase in the measured resistance of the thermal barrier layer after heat treatment at 1100  $^\circ\text{C}$ . This was linked to compositional changes in the layer itself. In this work, however, they were only able to compare the Bode plots with no attempt at geometrically correcting their data.

Previous modelling based on finite element (FE) has simulated the resistive surface layers on a substrate and provided some guidance on analysis [11]. An important factor is the electrode contact separation to electrode contact radius ratio,  $S/r$ . This can generate interference in current flow for low  $S/r$ , reducing the measured resistance of the material. It was estimated that reducing this interference effect required an  $S/r$  ratio of over 8x, which is challenging experimentally given the size of most samples. Veazey et al [11] also showed that for a surface layer which is 100 times more resistive than the bulk, if the layer is more than 10 times thinner than the contact radius ( $T/r < 0.1$ ), the most accurate method in calculating the surface layer conductivity,  $\sigma_s$ , is made using a modified geometric factor given by

$$\sigma_s = \frac{2T}{A_{mc}} \frac{1}{R} \quad (3)$$

shown schematically in Figure 2 (dashed red line). The thickness of the surface layer,  $T$  is now included in the correction, along with the surface area of the micro-contacts,  $A_{mc}$ . The sample resistance,  $R$  is measured from the impedance response. This assumes that the current acts linearly through the surface region but as the surface layer gets thicker compared to the micro contacts, the current profile can begin to spread in the surface region. The accuracy of this correction begins to decrease with increasing surface layer thickness [11] as shown in Figure 2, with increasing  $T/r$ .

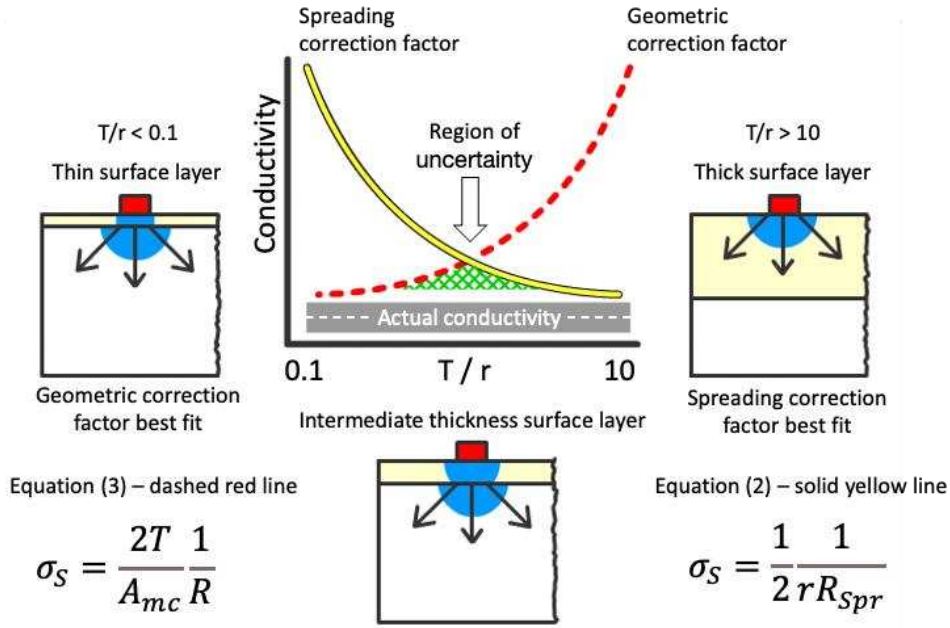


Figure 2. A schematic of how reliable the correction factors are for extracting conductivity of a surface layer compared to the actual conductivity (dashed white line) and 10% variation (grey region). This summarises the work in [11]. Yellow indicates a surface layer of thickness  $T$  and white indicates the bulk sample; note that only half the geometry for each configuration is shown due to symmetry. Blue indicates a region of higher current density with arrows indicating typical current flow. Samples with thin surface layers compared to the contact radius ( $T/r < 10$ ) are best corrected using the geometric correction factor (dashed red line). Conversely, for very thick layers ( $T/r > 10$ ), the spreading resistance correction provides the best estimate of the conductivity (solid yellow line). When the surface layer is of an intermediate thickness compared to the electrode radius, neither correction factor provides a good estimate as shown by the hashed green region.

Although the spreading resistance equation (2) can be relatively accurate for calculations based on a homogeneous material [15], when a resistive surface layer is included, this equation begins to overestimate  $\sigma_s$  for intermediate and thin surface layers with  $T/r < 10$ , as shown in Figure 2 (solid yellow line). Veazey et al proposed a choice between the two equations [11], with the spreading correction factor working well for  $T/r > 10$  and the geometric correction factor working well below  $T/r < 0.1$ ; however, this requires a decision to be made regarding which of the two is more appropriate and leads to a region of uncertainty for intermediate  $T/r$  values, as shown in Figure 2 (hashed green region).

To overcome this issue at intermediate  $T/r$  for resistive surface layers we propose a modified spreading resistance equation by replacing the factor of  $\frac{1}{2}$  in equation (2) with an appropriate correction factor (CF) to give

$$\sigma_s = CF \frac{1}{rR} \tag{4}$$

To understand how CF changes with  $T/r$ , we set the values of this ratio to be within the region of uncertainty in Figure 2 ( $0.125 < T/r < 3$ ). Using the conductivity and contact radius values assigned to the model, along with the resistance extracted from the

simulated impedance spectra, allows us to establish the appropriate correction factor ( $CF$ ) required to obtain accurate  $\sigma_s$  values. Thus, we can explore how to provide greater confidence and reliability in correcting measured resistances from mclS data of samples containing resistive surface layers under different sample/electrode ( $T/r$ ) arrangements.

### Model set-up

To construct a finite element representation of the problem we use a 3-dimensional cube of side length  $200 \mu\text{m}$ . We set the volume as an isotropic homogeneous material assigned with a conductivity  $\sigma = 13.6 \mu\text{S/m}$  and a relative permittivity of  $\epsilon_r = 162$ . These values were experimentally determined for a  $\text{SrTiO}_3$  single crystal sample at  $300^\circ\text{C}$  from conventional IS measurements [12]. A secondary layer of variable thickness to represent the resistive surface layer is then placed above this as shown in Figure 3.

Next, two circular areas, representing the electrode boundary conditions are placed on the upper surface with radius,  $r = 10 \mu\text{m}$ , as shown in figure 1. We denote the shortest distance between the electrode edges as the separation,  $S$ . Finally, we discretised this structure into tetrahedral elements (a finite element mesh) using the package Gmsh [13] and simulate the electrical response of dielectric materials using our in-house developed package Elcer with more details on this in the supplementary information and in [14].

To simplify the problem, we start with the micro-contact radii of all models to be  $r=10 \mu\text{m}$ , the side length of the model to  $200 \mu\text{m}$  and the relative permittivity of each layer to the bulk value of  $\epsilon_r = 162$ . The conductivity of the bulk layer is fixed at  $\sigma_b = 13.6 \mu\text{S/m}$ .

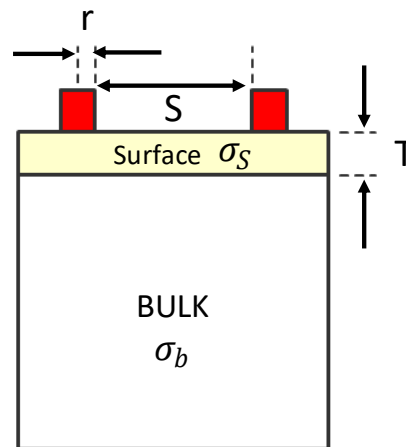


Figure 3. Illustration of the two-layer model used. It shows the key parameters such as micro-contact radius,  $r$ , surface layer thickness,  $T$ , and separation between the micro-contacts,  $S$ .

Using this model, we can study three key variables. First, the bulk-to-surface layer conductivity ratio ( $\sigma_b/\sigma_s$ ). Second, the thickness of the surface layer,  $T$ , and finally, the separation between the micro-contact electrodes,  $S$ . To encapsulate the variability that can arise in both the experimental configuration and material, we set ranges of these values.

The conductivity of the surface layer was set to range between  $\sigma_s=6.8 \mu\text{S/m}$  ( $\sigma_b/\sigma_s=2$ ) and  $\sigma_s=13.6 \text{ nS/m}$  ( $\sigma_b/\sigma_s=1000$ ). The surface layer thickness was modified between

$T=1.25$  and  $30\ \mu\text{m}$  with the electrode separation set to provide realistic  $S/r$  ratio values of 1, 4 and 8. Ratios of  $S/r=1$  and 4 were chosen as common practical settings when measuring fine features between two neighbouring microelectrodes. These lower  $S/r$  ratios however induce current interference between both electrodes and result in an overestimation of the conductivity [11]. The larger ratio we include of  $S/r=8$  has previously been reported to be the lowest separation required to obtain results within an acceptable  $\pm 10\%$  error range based on input values [11]. The surface layer to micro contact radius ratio ( $T/r$ ) is set to values of 0.125, 0.25, 0.5, 1, 2 and 3.

#### Determining the value of CF using equation (4)

To help identify the surface layer response through all our simulated responses, we first analyse the electrical response of a homogenous model where the surface layer has the same conductivity as the bulk,  $\sigma_b/\sigma_s=1$ , that is a pure 'bulk' model. As shown in figures 4(a) and (b), the simulated response based on spectroscopic plots of the imaginary component of the complex impedance,  $-Z''$ , and the electric modulus,  $M''$ , result in a single peak for each  $S/r$  ratio with  $f_{\text{max}}=1.53\ \text{kHz}$ , agreeing well with the theoretical value of  $1.50\ \text{kHz}$  (based on the relationship  $\omega RC=1$  with  $\omega = 2\pi f_{\text{max}}$ , and  $f_{\text{max}}$  being the frequency at the top of the  $-Z''$  and  $M''$  Debye peaks). The  $-Z''$  peak height increases with increasing  $S/r$  (also shown for  $Z^*$  plots in SI-figure 1) indicating an increase in sample resistance whereas the decrease in height of the corresponding  $M''$  peak indicates an increase in capacitance. For  $S/r=30$ , a  $-Z''$  peak height of  $1.78\ \text{G}\Omega$  is obtained but decreases to  $1.40\ \text{G}\Omega$  for  $S/r=1$ . As  $f_{\text{max}}$  does not change in either the  $-Z''$  or  $M''$  spectra, the changes in capacitance ( $C$ ) and resistance ( $R$ ) are influenced by the separation between the electrodes. For all simulations presented here, the bulk properties are fixed and this allows the bulk response to be identified in the  $-Z''$  and  $M''$  spectra, through its  $f_{\text{max}}$  value of  $1.5\ \text{kHz}$ .

We can now illustrate how we use this electrical response to determine CF for a specific configuration. We employ this on a series of simulations for a resistive surface layer based on  $\sigma_b/\sigma_s = 100$ ,  $S/r = 4$  and various surface layer thicknesses. The simulated  $-Z''$  spectra are shown in figure 4(c) and display a single Debye peak at  $f_{\text{max}} = 15\ \text{Hz}$  which increases in height as the surface layer thickness is increased. The reduction in  $f_{\text{max}}$  value by a factor of 100 compared to the homogeneous model is consistent with the reduced conductivity of the surface layer. The  $-Z''$  spectra are therefore dominated by the response from the surface layer, our region of interest. The expected  $f_{\text{max}}$  values for the conductivity ratios used throughout the article are summarised in Table 1 of the SI.

The corresponding spectroscopic plots of the imaginary component of the electric modulus,  $M''$  are shown in Figure 4(d) and reveal two distinct Debye-peak type responses. This illustrates the influence of volume fraction associated with the bulk and surface layer regions based on the thickness of the surface layer. The lower frequency peak at  $15\ \text{Hz}$  associated with the surface layer increase in height (and therefore volume fraction) with increasing surface layer thickness; however, the higher frequency peak at  $1.5\ \text{kHz}$  associated with the bulk response decreases in height (and therefore volume fraction) as the surface layer thickness is increased. Although the  $M''$  spectra illustrate that both the surface and bulk regions are being probed in the mCIS simulations, the  $-Z''$  spectra in Figure 4 (c) illustrate that in models for  $\sigma_b/\sigma_s = 100$ , the complex impedance data are dominated by the response of the surface layer.

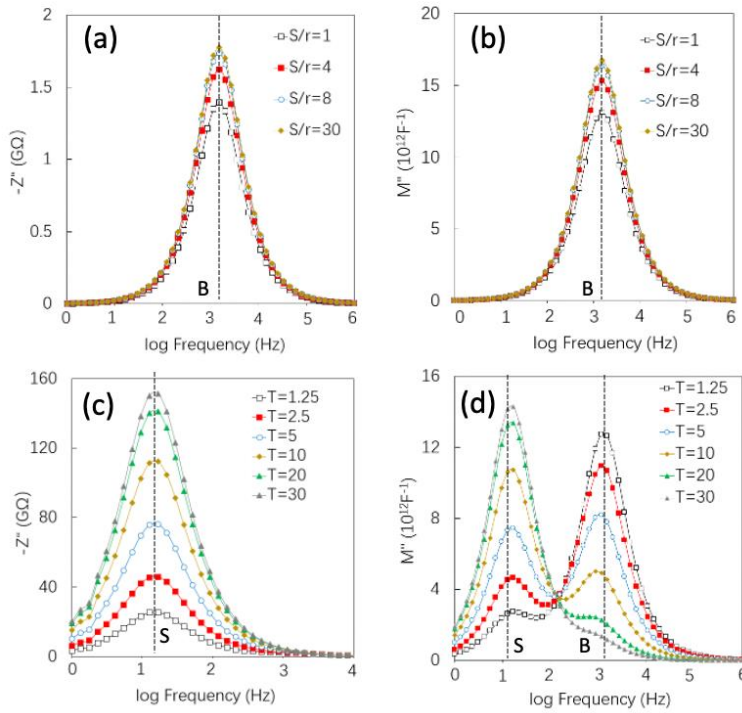


Figure 4. The simulated impedance spectra overlaid with dashed black lines highlighting the expected  $f_{max}$  values for the surface (S) and bulk (B). Parts (a) and (b) shows the  $-Z''$  and  $M''$  spectra for a homogenous model with  $\sigma_b/\sigma_s=1$  for various  $S/r$  ratios. A single peak at 1.5 kHz is observed representing the bulk response. In (c) and (d) the simulated impedance spectra for when  $\sigma_b/\sigma_s = 100$  is shown for the  $-Z''$  and  $M''$  spectra, respectively. In  $-Z''$  a single peak is observed at 15 Hz representing the surface, however in  $M''$  both the surface and bulk responses can be observed.

The resistance  $R$  of the surface layer in the heterogeneous models is obtained using the  $-Z''$  peak,  $Z''_{max}$  in figure 4(c) via equation 5

$$R = -2Z''_{max} \quad (5)$$

Equation 4 is then used to determine the correction factor required to provide the correct conductivity for each model.

## Results

To understand how the correction factor is altered by changes in the surface layer, three key ratios are investigated. These are the  $S/r$  ratio dealing with contact separation; the  $\sigma_s/\sigma_b$  ratio to identify how surface layer conductivity alters the response; and the  $T/r$  ratio which investigates the influence of surface layer thickness. For completeness, we also investigate how the contact radius  $r$  influences  $CF$ .

We start the process of investigating  $CF$  values using a homogenous model without a surface layer. We simulate the case when  $\sigma_s=\sigma_b$  ( $\sigma_s/\sigma_b=1$ ) for  $S/r = 1, 4$  and  $8$ . With

these properties, the model represents an isotropic homogenous material with no surface layer. Therefore, the  $CF$  value extracted for these models should be close to the factor of  $\frac{1}{2}$  in equation (2). This is the case for  $S/r=8$  which agrees well with an extracted  $CF = 0.47$ . This is due to the distance between the contacts generating limited overlap (interference) of the high current densities. Veazey et al suggested that if the error requirement is to be within  $\pm 10\%$  of the assigned conductivity, the  $S/r$  ratio can be reduced to 8 [11], and our results are therefore consistent with this. For the case of  $S/r = 4$  and 1, overlapping of the high current density zones underneath the electrodes becomes significant and produces increasing current density (and therefore interference). Consequently, the resistance of the material is underestimated and therefore increases the error  $>10\%$  and reduces  $CF$  to 0.38 for  $S/r = 1$ .

Now that changes due to interference have been identified, we can establish how changes in the surface layer conductivity alters  $CF$  by creating a series of models where the surface layer is now 100x more resistive than the bulk. Again,  $S/r$  values are 1, 4 and 8. The calculated  $CF$  values extracted from the simulated impedance (see SI) results are shown in Figure 5. It highlights that when  $T/r$  is low, the  $CF$  value for all three  $S/r$  sets also remains low,  $\sim 0.1$ . As  $T/r$  increases,  $CF$  for the 100x case for all  $S/r$  ratios also increases. Above  $T/r = 1$ , the individual responses start to separate as they increase towards their corresponding homogeneous model. At that point, when the surface layer is thick enough, the impedance response should be similar to a single-layer model with homogenous surface layer material properties, as was schematically shown in Figure 2 (solid yellow line). As shown in Figure 5, there is relatively little change in the  $CF$  value with respect to the  $S/r$  ratios across the range of  $T/r$  range investigated here. Furthermore, for various radii (see supplementary figure 5), the results overlay well, indicating that  $CF$  is insensitive to changes in this micro-contact radius range.

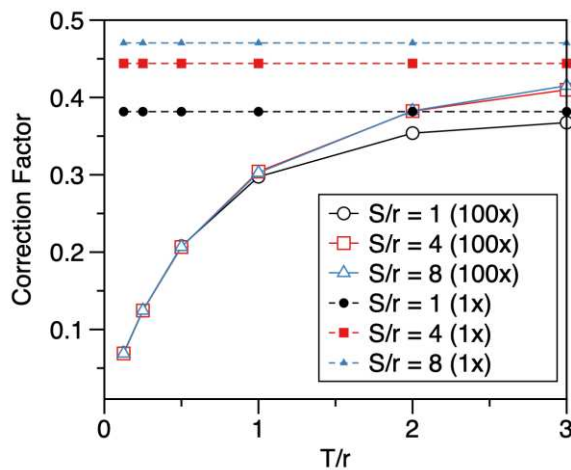


Figure 5. Correction factor ( $CF$ ) against surface thickness/micro contact radius ( $T/r$ ) for different  $\sigma_b/\sigma_s$  ratios and  $S/r$  ratios of 1, 4 and 8. The 1x set ( $\sigma_b/\sigma_s$ ) is shown with dashed lines and filled symbols, whereas the 100x models ( $\sigma_b/\sigma_s=100$ ) are shown as open symbols.

We now expand the applicability to changes in  $\sigma_b/\sigma_s$ . Experimentally, various  $\sigma_b/\sigma_s$  ratios are likely to occur and it is instructive to explore how this influences  $CF$ . Generated impedance results for different  $\sigma_b/\sigma_s$  models were obtained (see SI figures (2-4) for complete set of results) and the associated  $CF$  values calculated are shown in Figure 6. We start by reducing the ratio of  $\sigma_b/\sigma_s$  from 100x to 10x leading to the surface layer's properties being set to  $\sigma_s=1.36 \mu\text{Sm}^{-1}$  and  $\epsilon_r = 162$ . The same previous sets of  $S/r = 1, 4$  and 8 were studied. In each case, the surface layer thickness was

increased from  $T=1.25$  to  $30\ \mu\text{m}$  to maintain the  $T/r$  range previously used. For ease of comparison, only results of  $S/r=4$  for  $\sigma_b/\sigma_s=10$  are shown but others follow the same trend (see SI) and the results are compared against the previous  $\sigma_b/\sigma_s=100$  values, Figure 6(a). The  $CF$  trend for  $\sigma_b/\sigma_s=10$  shows a small downward translation compared to that for  $\sigma_b/\sigma_s=100$  for all  $T/r$  values which can be attributed to the increased contribution from the bulk response. This is also shown in the  $-Z''$  spectra (see Figure 6(b) and SI Figure 3 for other  $S/r$  ratios) where a small, secondary peak associated with the bulk response can now be observed near 1.5 kHz. The  $f_{\text{max}}$  values match well to the expected surface layer  $f_{\text{max}}$  of 153 Hz through the  $T/r$  range with relatively little change in  $CF$  based on  $r=10\ \mu\text{m}$  (see SI figure 6). We also note that where low  $T/r$  generates low  $CF$  values which increase as  $T/r$  increases, but for all  $r$  values used they overlay well which indicates that  $CF$  is insensitive to changes in this micro-contact radius range.

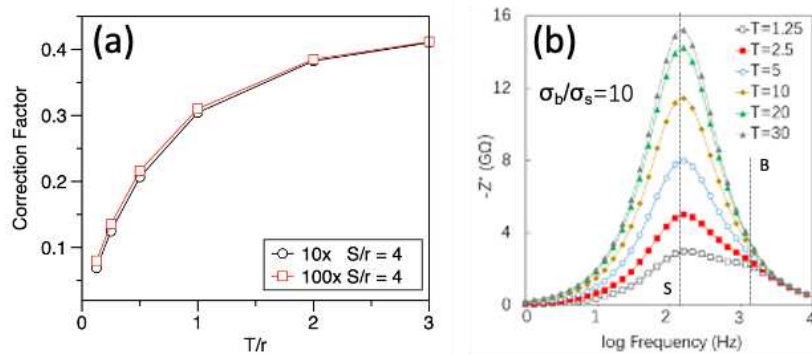


Figure 6. (a) Correction factor ( $CF$ ) versus  $T/r$  for models of  $\sigma_b/\sigma_s=10$  and  $\sigma_b/\sigma_s=100$ , both have  $S/r$  ratio of 4. A small upshift of  $CF$  value for  $\sigma_b/\sigma_s=10$  occurs across the entire  $T/r$  range. (b)  $-Z''$  spectra for  $\sigma_b/\sigma_s=10$  at  $S/r=4$ .  $f_{\text{max}}$  of the surface response changes with layer thickness and a secondary peak at  $\sim 1.5$  kHz starts to be observed at low  $T$  values as the bulk impedance response becomes increasingly significant. This is overlaid with dashed black lines highlighting the expected  $f_{\text{max}}$  values for the surface (S) and bulk (B) responses.

We now reduce the conductivity difference further to  $\sigma_b/\sigma_s=5$  ( $\sigma_s=6.78\ \mu\text{Sm}^{-1}$ ) shown in figure 7. Analysis of the  $\sigma_b/\sigma_s=5$  models for the  $CF$  are shown in Figure 7(a). The case of  $\sigma_b/\sigma_s=100$  at  $S/r=4$  is included as a reference for a case where the impedance data show no  $f_{\text{max}}$  deviation(s). The  $CF$  across all  $S/r$  ratios for  $\sigma_b/\sigma_s=5$  is very similar to the  $\sigma_b/\sigma_s=100$  models. Although the numerical difference between the 100x and 5x trends when  $S/r=4$  is relatively large when the  $T/r$  value is low, they converge toward the 100x when  $S/r=4$  as the surface layer thickness increases. This coincides with the degree of  $f_{\text{max}}$  deviation observed in the  $\sigma_b/\sigma_s=5$  models, figure 7(b) and supplementary figure 7. We note at low values of  $T/r$  the value of  $f_{\text{max}}$  lays between the intrinsic values expected for the individual surface and bulk values shown in figure 7(b) and in SI Table 1 and figure 7. The deviation from the intrinsic values for the bulk and surface layer highlight that these values are not representative of charge conduction through an individual material but a consequence of the  $f_{\text{max}}$  values being different but of similar magnitude for the bulk and surface layer materials. This arises due to a limitation in the resolution limits of impedance spectroscopy.

At these values the  $-Z''$  spectra can contain significant contributions from both bulk and surface regions, as shown in Figure 7(b). When the surface layer is thin, the  $f_{\text{max}}$  deviation in the  $-Z''$  spectra is large but decreases with increasing surface layer thickness. For example, for  $S/r=4$  and where the surface layer is relatively thin ( $T=1.25\ \mu\text{m}$ ),  $f_{\text{max}}$  for the  $-Z''$  Debye peak is 650 Hz which is significantly higher than the 300 Hz

expected based on the theoretical value for the surface layer properties. This degree of deviation in  $f_{\max}$  of the  $-Z''$  peak reduces as the surface layer thickness is increased due to the bulk region being further from the high current density of the electrodes. At  $T=10\ \mu\text{m}$ ,  $f_{\max}$  is 281 Hz indicating the contribution from the bulk to the overall  $-Z''$  response is low.

It is noteworthy there is a notable difference in the  $CF$  trend when  $T/r$  increases for 5x when  $S/r=1$ . This can be attributed to the consequence of high current interference between the closely placed electrodes and the same trend is observed in Figure 5 for  $\sigma_b/\sigma_s=100$ .

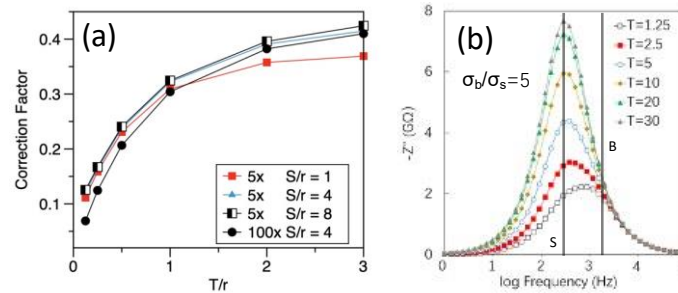


Figure 7. (a) Correction factor ( $CF$ ) trends for  $\sigma_b/\sigma_s = 5$  models with  $S/r$  ratios of 1, 4 and 8. The 100x trend for  $S/r=4$  is plotted as a reference to investigate the influence of decreasing  $\sigma_b/\sigma_s$  ratio on  $CF$ . A deviation from the 100x  $S/r=4$  trend occurs when the  $T/r$  value is low. (b) The impedance response for  $S/r = 4$  where  $f_{\max}$  of the  $-Z''$  peak (predominantly associated with the surface response) changes with layer thickness. This is overlaid with dashed black lines highlighting the expected  $f_{\max}$  values for the surface (S) and bulk (B) responses.

In this work, we show that a modified spreading resistance equation can provide greater reliability in geometrically correcting for resistive surface layers through modification of a correction factor,  $CF$ . This works well when  $\sigma_b/\sigma_s$  is  $> 10x$ . As the ratio  $\sigma_b/\sigma_s$  reduces, the time constants of the two layers begin to overlap and resolving the individual responses becomes more challenging. This is also reflected in  $CF$ , as the values measured using  $\sigma_b/\sigma_s = 10$  and 5 deviate from those measured for  $\sigma_b/\sigma_s = 100$ . Therefore, it is important to have an expectation of the differences in time-constant between the two layers. This is possible when creating a desired coating or thin film on a substrate, as the properties of the bulk and surface layers could be examined individually by conventional impedance spectroscopy. Thus, if the  $\sigma_b/\sigma_s$  ratio is larger than 100x, then the correction should have relatively high reliability.

It is challenging however in retrieving the surface layer thickness in situations when damage or degradation of the surface is involved. In such cases, transmission electron microscopy may be needed first to estimate the thickness of a surface layer and to establish if the layer thickness is homogenous across the sample. If  $T/r$ ,  $S/r$  and  $\sigma_b/\sigma_s$  can be estimated, then this modified spreading resistance equation method can then be applied to extract surface layer conductivity and other electrical properties with a higher degree of accuracy compared to the original top-top spreading resistance equation (2). If the surface layer is inhomogeneous however, for example, being functionally graded or the interface is highly rough or discontinuous with the bulk material this could severely limit the use of mclS to extract meaningful results. In such cases, selecting an appropriate correction factor would be non-trivial.

## Conclusions

We have developed a FEM for top-top microcontacts on a resistive surface layer linked to simulated impedance spectroscopy data to show how a modification of the spreading resistance correction equation can improve the accuracy of extracting the conductivity of the resistive surface layer. This does not require switching between the geometric and conventional spreading resistance correction equations as previously suggested. When the  $\sigma_b/\sigma_s$  ratio is  $\sim 100$  or greater, the surface layer conductivity can be calculated for typical T/r ratios employed in mCIS experiments. When the  $\sigma_b/\sigma_s$  ratio is less than 100, only when the surface layer thickness to electrode radius ratio (T/r) is larger than 3 can the surface layer conductivity be estimated to within 10% accuracy.

## References

- [1] J. T. S. Irvine, D. C. Sinclair and A. R. West, "Electroceramics: Characterization by Impedance Spectroscopy," *Adv. Mater*, **2**,132–138, 1990.
- [2] D. C. Sinclair and A. R. West, "Impedance and modulus spectroscopy of semiconducting barium titanate showing positive temperature coefficient of resistance," *J Appl Phys*, **66**, 3850–3856, 1989.
- [3] S. I. Costa, M. Li, J. R. Frade and D. C. Sinclair, "Modulus spectroscopy of  $\text{CaCu}_3\text{Ti}_4\text{O}_{12}$  ceramics: clues to the internal barrier layer capacitance mechanism," *RSC Advances*, **3**, 7030–7036, 2013.
- [4] R. Holm, *Electric Contacts*, Springer, 1967.
- [5] J. Fleig and J. Maier, "Local conductivity measurements on AgCl surfaces using microelectrodes," *Solid State Ionics*, **85**, 9–15, 1996.
- [6] J. Fleig, "Microelectrodes in solid state ionics," *Solid State Ionics*, **161**, 279–89, 2003.
- [7] E. Navickas, M. Gerstl, G. Friedbacher, F. Kubel and J. Fleig, "Measurement of the across-plane conductivity of YSZ thin films on silicon," *Solid State Ionics*, **211**, 58–64, 2012.
- [8] J.-H. Joo and G.-M. Choi, "Electrical conductivity of YSZ film grown by pulsed laser deposition," *Solid State Ionics*, **177**, 1053-1057, 2006.
- [9] D.-H. Zhang, H.-B. Guo and S.-K. Gong, "Impedance spectroscopy study of high-temperature oxidation of  $\text{Gd}_2\text{O}_3$ - $\text{Yb}_2\text{O}_3$  codoped zirconia thermal barrier coatings," *Trans. Nonferrous Met. Soc. China*, **21(5)**, 1061-1067, 2011.
- [10] M. Shirpour, R. Merkle and J. Maier, "Space charge depletion in grain boundaries of  $\text{BaZrO}_3$  proton conductors," *Solid State Ionics*, **225**, 304-307, 2012.
- [11] R. A. Veazey, A. S. Gandy, D. C. Sinclair and J. S. Dean, "Finite element modeling of resistive surface layers by micro-contact impedance spectroscopy," *J Am Ceram Soc*, **103**, 2702– 2714, 2020.
- [12] R. A. Veazey, A. S. Gandy, D. C. Sinclair and J. S. Dean, "Modeling the influence of two terminal electrode contact geometry and sample dimensions in electro-materials," *J Am Ceram Soc*, **102**, 3609– 3622, 2019.
- [13] C. Geuzaine and J. Remacle, "Gmsh: a three-dimensional finite element mesh generator with built-in pre- and post-processing facilities," *Int. J. Numer. Methods Eng*, **79**, 1309-1331, 2009.
- [14] J. S. Dean, J. H. Harding and D. C. Sinclair, "Simulation of Impedance Spectra for a Full Three-Dimensional Ceramic Microstructure Using a Finite Element Model," *J. Am. Ceram. Soc*, **97**, 885-891, 2013.

[15] J. Fleig, in *Advances in Electrochemical Science and Engineering*, Wiley-VCH, 2002, 1-79.

Supplementary Information

Additional details on the modelling

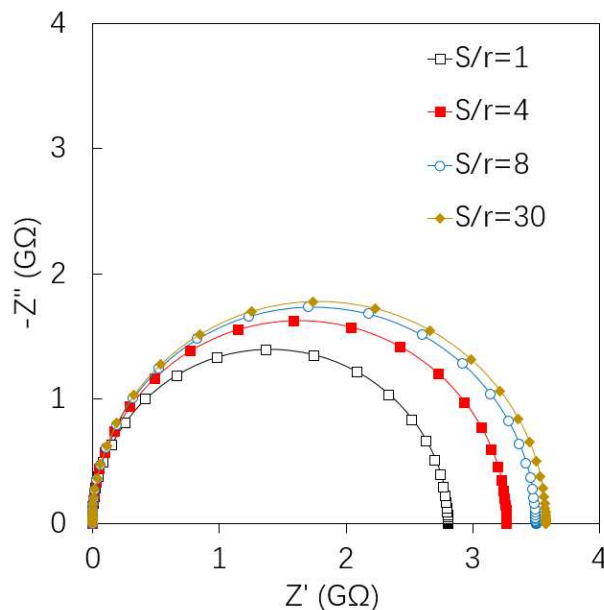
The modelling presented here used Elcer; this is based on a finite element technique using a time domain finite element method (TDFEM) to solve Maxwell's equations in space and time. The microstructure of the system can then be represented in three dimensions with individual volumes. These different regions possess an individual conductivity ( $\sigma$ ) and relative permittivity ( $\epsilon_r$ ) simulating an electrical heterogeneity within the model without the need for equivalent circuits and constant phase elements. The model is then meshed using Gmsh and solved using Elcer.

We use Dirichlet boundary conditions at the electrode–air interface to fix the electric potential and assume displacement currents crossing the free surface of the material are zero by using Neumann boundary conditions.

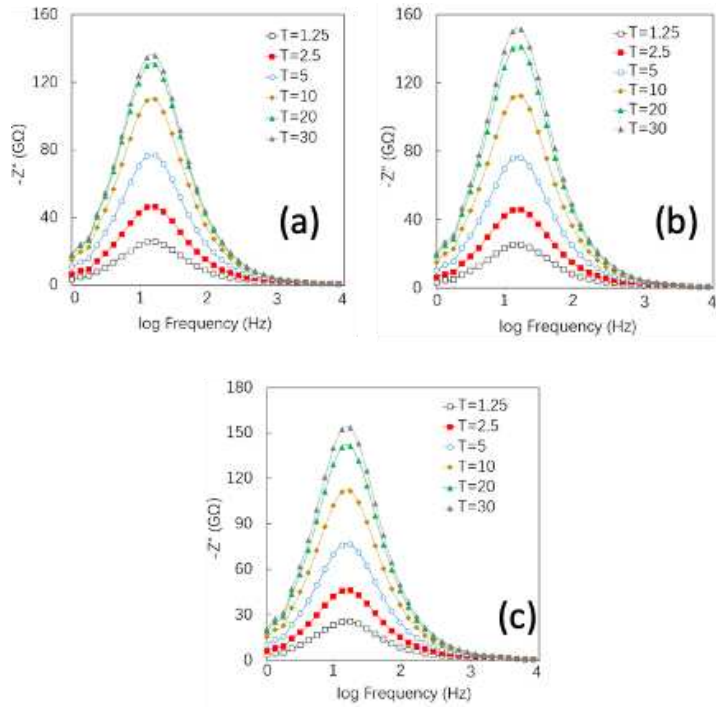
In the simulations presented here we consider a frequency range 1 Hz – 1 MHz using a potential of 0.1 V applied on a contact region set with conductivity of 10 kS/m, representing the electrode material.

Table S1 the expected  $f_{\max}$  values for the surface conductivities and ratios used. Note the bulk conductivity is fixed in all systems at  $13.6 \times 10^{-6}$  S/m.

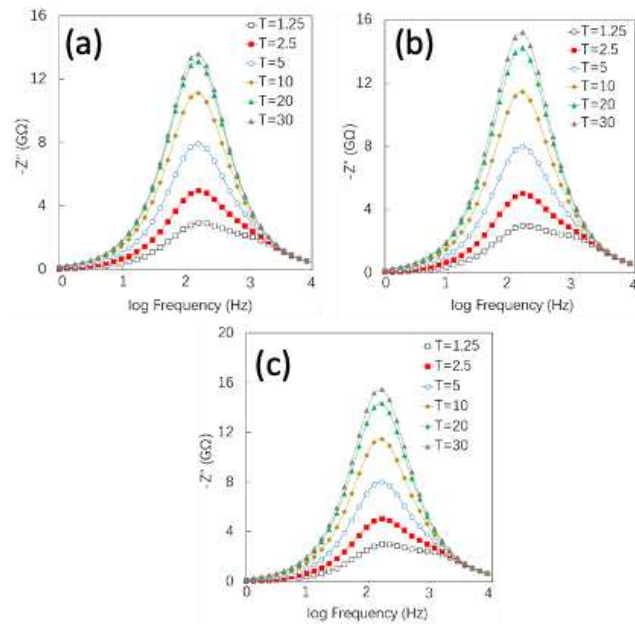
Surface Conductivity S/m	Conductivity ratio ( $\sigma_b/\sigma_s$ )	Expected $f_{\max}$ Hz
$13.6 \times 10^{-6}$	1	1530
$2.72 \times 10^{-6}$	5	306
$13.6 \times 10^{-7}$	10	153
$13.6 \times 10^{-8}$	100	15.3
$13.6 \times 10^{-9}$	1000	1.53



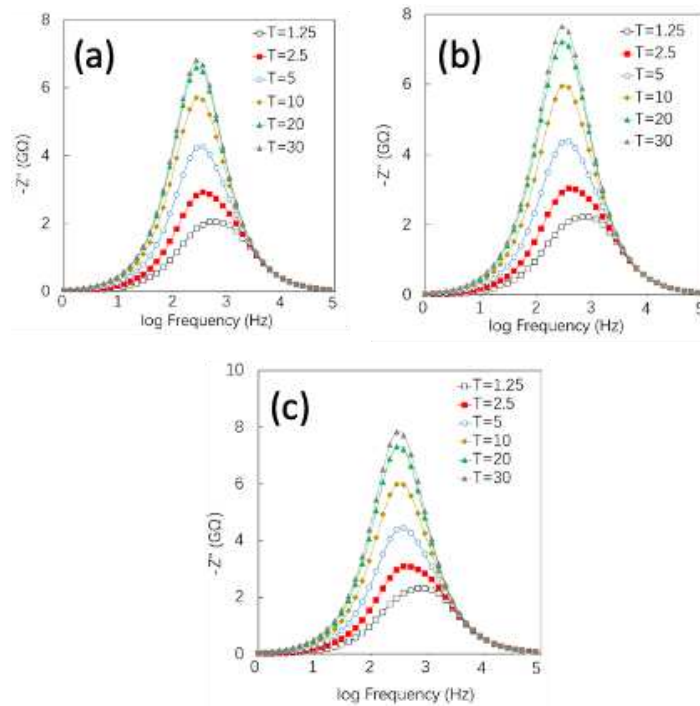
Supplementary figure 1. Complex Impedance,  $Z^*$ , plots of the homogenous model for various S/r ratios.



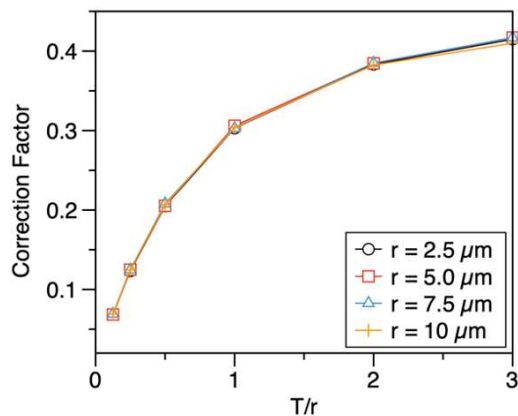
Supplementary Figure 2. Simulated  $Z''$  spectra for  $\sigma_b/\sigma_s=100$  with (a)  $S/r=1$ , (b)  $S/r=4$  and (c)  $S/r=8$ .



Supplementary Figure 3. Simulated  $-Z''$  spectra for  $\sigma_b/\sigma_s=10$  with (a)  $S/r=1$ , (b)  $S/r=4$  and (c)  $S/r=8$ .

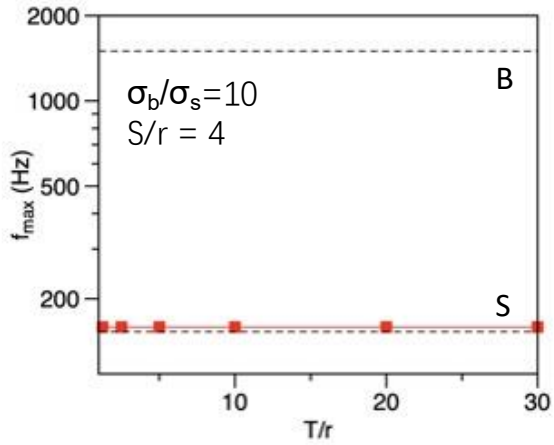


Supplementary Figure 4. Simulated  $Z''$  spectra for  $\sigma_b/\sigma_s=5$  with (a)  $S/r=1$ , (b)  $S/r=4$  and (c)  $S/r=8$

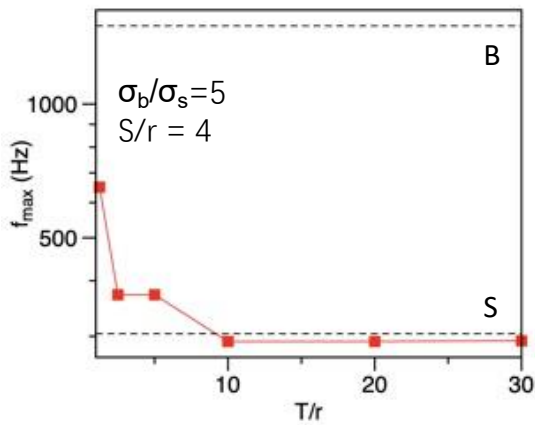


Supplementary Figure 5 (a) Correction factor ( $CF$ ) versus  $T/r$  for models with different micro contact radii of 2.5, 5, 7.5 and 10  $\mu\text{m}$ . All models have  $\sigma_b/\sigma_s = 100$  and  $S/r = 4$  and are shown to be superimposed upon each other.

Through this  $T/r$  range however, there is relatively little change in  $CF$  based on  $r = 10 \mu\text{m}$ . To test the generality of this approach, we varied the contact radius. This is an important parameter to quantify as it is something that will vary between different research groups depending on their electrode fabrication facilities.  $CF$  values for four different microcontact radii, ranging from 2.5 to 10  $\mu\text{m}$ , are shown in Supplementary Figure 5 for the conditions  $\sigma_b/\sigma_s = 100$  and  $S/r = 4$ . A similar trend to Figure 5 (main article) is observed, where low  $T/r$  generates low  $CF$  values which increase as  $T/r$  increases, but for all  $r$  values used they coincide well which indicates that  $CF$  is insensitive to changes in this micro-contact radius range.



Supplementary figure 6.  $f_{\max}$  values extracted from figure 6(b) in the main script highlight the insensitive response as a function of  $T/r$  for  $\sigma_b/\sigma_s = 10$  and  $S/r = 4$ . The expected  $f_{\max}$  values for the surface (S) and bulk (B) responses are shown as dashed lines.



Supplementary figure 7.  $f_{\max}$  values extracted from figure 7(b) in the main script highlighting how  $f_{\max}$  changes with increasing  $T/r$  ratio for  $\sigma_b/\sigma_s = 5$  and  $S/r = 4$ . The expected  $f_{\max}$  values for the surface (S) and bulk (B) responses are shown as dashed lines. There is a clear difference at low  $T/r$  ratio, due to a combined response from the surface and bulk. The  $f_{\max}$  values tend towards  $\sim 10\%$  of the expected surface value for  $T/r \geq 10$